Symmetry-broken crystal structure of elemental boron at low temperature

M. Widom
Department of Physics, Carnegie Mellon University, Pittsburgh, Pennsylvania 15213, USA

M. Mihalkovič
Institute of Physics, Slovak Academy of Sciences, Bratislava, Slovakia

(Received 11 September 2007; revised manuscript received 6 November 2007; published 25 February 2008)

The crystal structure of boron is unique among chemical elements, highly complex, and imperfectly known. Experimentalists report that the β-rhombohedral (black) form is stable over all temperatures from absolute zero to melting. However, early calculations found its energy to be greater than the energy of the α-rhombohedral (red) form, implying that the β phase cannot be stable at low temperatures. Furthermore, the β form exhibits partially occupied sites, seemingly in conflict with the thermodynamic requirement that entropy vanish at low temperature. Using electronic density functional theory methods and an extensive search of the configuration space we find a unique, energy-minimizing pattern of occupied and vacant sites that can be stable at low temperatures but that breaks the β-rhombohedral symmetry. Even lower energies occur within larger unit cells. Alternative configurations lie nearby in energy, allowing the entropy of partial occupancy to stabilize the β-rhombohedral structure through a phase transition at moderate temperature.

DOI: 10.1103/PhysRevB.77.064113 PACS number(s): 61.66.Bi

I. INTRODUCTION

Elemental boron is important for its light weight, high strength, high melting point, and semiconducting properties. It is also intrinsically interesting owing to its complex structures, which are characterized by their arrangements of icosahedral clusters. Boron is almost unique among elements in lacking a well-understood and universally agreed upon low-temperature structure. Knowledge of the precise structure is required for understanding its remarkable electronic and mechanical properties, and also for understanding the stability of technologically important boron compounds relative to their constituent elements.

The first reported crystallographic refinements of elemental boron were the α-tetragonal[1,2] and α-rhombohedral forms.[3,4] Although the α-rhombohedral form was initially believed stable at low temperature,[3] the β-rhombohedral form was later discovered[5] and proposed as the true low-temperature state. Still later, the β-tetragonal form was discovered and its crystal structure refined.[6] The α- and β-rhombohedral structures are illustrated in Figs. 1 and 2 and are described in greater detail in Sec. I A.

The debate over the proper stable form of boron continues today, with some researchers suggesting the α-rhombohedral form as the true low-temperature state.[7] In particular, the calculated energy of the α form lies below the reported calculated energies of the β form.[7–10] Some researchers propose a finite-temperature phase transition,[11] including one proposal that vibrational entropy drives an α to β transition at finite temperature.[7] Quantum mechanical zero-point vibrational energy has been proposed as a mechanism to stabilize the β-rhombohedral form at absolute zero.[10]

We note that the β-rhombohedral form exhibits intrinsic disorder in the form of partially occupied sites. Partial occupancy occurs in crystallographic refinement when the site is occupied, at a given instant, in some copies of the unit cell but not in others. Within a single unit cell the site may be occupied at some times but not at others. Since thermodynamics requires that entropy vanish in the limit of low temperature, and partial occupancy implies finite entropy, the partially occupied β-rhombohedral form is not a plausible low-temperature structure. Correlations among the partially occupied sites of the β form must favor a unique pattern of occupancy that minimizes the energy.

We carry out an extensive study of the configuration space that explores specific resolutions of partial occupancy, assigning atoms or vacancies to specific sites. Our results (see Table I) indicate that a particular symmetry-broken form of β-boron achieves energy lower than the α form and thus is the true low-temperature structure. A symmetry-restoring phase transition, driven by the high entropy of an ensemble of nearly degenerate configurations, should occur at a moderate temperature, explaining the experimental observation of the β-rhombohedral form as the equilibrium phase at higher temperatures.

The remainder of this introduction briefly describes the known structures of crystalline boron and our calculational methods. Results are presented in Sec. II. We find optimal assignments of atoms to partially occupied sites, we validate

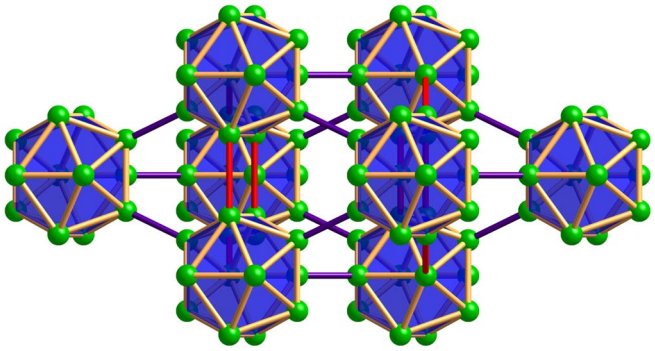

FIG. 1. (Color online) Structure of α-rhombohedral boron viewed along the rhombohedral $(11\bar{2})$ axis. Bond color scheme: 1.67 Å in purple; 1.75–1.81 Å in orange; 2.01 Å in red.

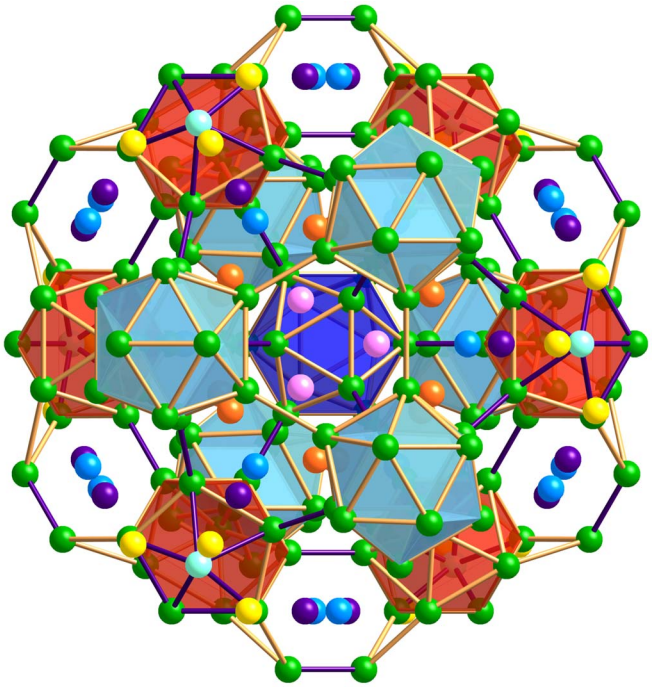

FIG. 2. (Color online) Structure of β-rhombohedral boron viewed along rhombohedral (111) axis. Bond color scheme: 1.63–1.73 Å in purple; 1.73–1.92 Å in orange. Partially occupied sites (see text) are shown in color: B13 (74.5% average occupancy) cyan; B16 (27.2%) pink; B17 (8.5%) yellow; B18 (6.6%) indigo; B19 (6.8%) blue; B20 (3.7%) orange.

these findings using solid state molecular dynamics simulations, and we explore possible superlatttice ordering. Finally we discuss our conclusions in Sec. III.

A. Structural description

Crystalline boron occurs primarily in tetragonal and rhombohedral forms. Since the tetragonal forms are known to be metastable, our analysis in this paper focuses on the rhombohedral forms. Both the α- and β-rhombohedral forms share a common space group $R\bar{3}m$ (group no. 166). Three rhombohedral primitive cells combine to form a larger nonprimitive hexagonal unit cell with three times the number of atomic sites. The rhombohedral (111) axis becomes the hexagonal symmetry axis of the hexagonal unit cell. For simplicity, our analysis is based on the rhombohedral primitive cell, though we do at the end consider supercells of the primitive cell including the full hexagonal unit cell.

Structure types are denoted by their Pearson symbols. For example, Pearson type $tP50$ (α-tetragonal) is primitive tetragonal with 50 atomic sites per cell. Pearson $tP196$ (β-tetragonal) is also primitive tetragonal but with 196 atomic sites per unit cell. Because of partial occupancy $tP196$ actually has fewer than 196 atoms distributed among its 196 sites. Pearson $hR12$ (α-rhombohedral) and $hR105$ (β-rhombohedral) are both rhombohedral primitive cells of 12 and 105 sites, respectively. Three rhombohedral primitive cells may be combined to form a single hexagonal cell.

All crystalline boron structures share a common structural motif, the 12-atom icosahedral cluster. Various allotropes differ in the spatial arrangement of the icosahedra and in the presence of interstitial atoms. The structural complexity of boron is due to the "electron deficiency" of the B_{12} icosahedral cluster[12,13] which frustrates the distribution of electrons among available bonds. Presumably the partial site occupancy serves to relieve this frustration.[14]

Among boron allotropes, α-rhombohedral boron has the simplest structure (see Fig. 1), with a B_{12} icosahedral cluster placed at each vertex of the rhombohedral cell. The structure is defined by just two independent Wyckoff positions.[15] The icosahedral clusters are nearly regular, with bond lengths in the range of 1.75–1.81 Å. Clusters are joined along 6 of their 12 fivefold axes that point radially outward through vertices of the icosahedron. These intericosahedral bonds have length 1.67 Å. Also visible in the figure are bonds of length 2.01 Å running parallel to the icosahedral twofold axes. This bond length is almost completely absent in all other allotropes, so we believe it is energetically unfavorable.

The β-rhombohedral structure (see Fig. 2) differs from the α in that the icosahedral cluster at the origin joins to 12 other icosahedra along each of its 12 fivefold axes. In contrast to the α structure, where all icosahedra share a common orientation, in the β form the 12 surrounding icosahedra are each rotated by 36° relative to the central icosahedron around their common axes. Consequently, the lattice constant of the β structure is approximately double that of the α. As shown, the icosahedra shaded in blue are at positions equivalent to those in the α structure, while those shaded in red are new.

Another new feature in the β form is the presence of partially occupied sites. Although the original $hR105$ structure model[5,16] contained 15 Wyckoff positions, each fully occupied, an intermediate model[17,18] (Pearson type $hR111$) assigned the B13 position 73% average occupancy and introduced a new B16 position at 25% occupancy (the numbering scheme we use is common to all the cited authors). In the Pearson type $hR141$ model[19] illustrated in Fig. 2, the B13 position is listed at 74.5% average occupancy, the B16 position at 27.2%, and additional positions B17, B18, B19, and B20 are given occupancies of 8.5%, 6.6%, 6.8%, and 3.7%, respectively. Other than the B20 position, all partially occupied positions lie in mirror planes of the structure that contain the rhombohedral (111) axis. They appear as collinear sets in the projection shown in Fig. 2.

B. Methods

Our basic calculational methods follow Ref. 8. The calculations use the electronic density functional program[20] VASP version 4.6.28. VASP uses a plane-wave approach that relies on periodic boundary conditions and is well suited to the study of periodic crystal structures. Electron-ion interactions are represented using projector augmented wave (PAW) potentials,[21,22] which are an all-electron generalization of pseudopotentials. For boron the 1s electrons are treated within the ionic core while the 2s and 2p electrons are assigned to the valence band. All structures considered were electrically neutral.

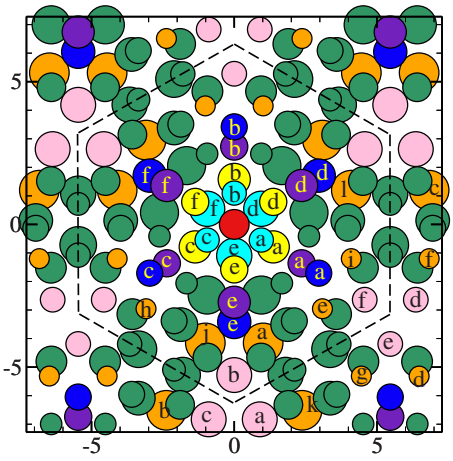

FIG. 3. (Color online) Structure of β-rhombohedral boron in vicinity of cell body center (B15, shown in red) viewed along the rhombohedral (111) axis. Color coding as in Fig. 2 (radially outward from center: B13 cyan; B17 yellow; B18 indigo; B19 blue; B16 pink. Other atoms are green except for B20 in orange). Site labels correspond to notation in Table III. Size of atoms indicates vertical position, with small on top. Length scale is in angstroms. The dashed lines contains a single hexagonal unit cell.

The exchange-correlation functional is taken as the Perdew-Wang 1991 (PW91) generalized gradient approximation (GGA).[23] Previously the GGA has been shown superior to the local density approximation (LDA) for studies of boron clusters and compounds,[24,25] with accuracy nearly that of Hartree-Fock calculations at the self-consistent-field level.[26]

All structures are fully relaxed, in both atomic coordinates and lattice parameters, subject to the preservation of initial symmetry, using a conjugate gradient algorithm. Owing to coupling of the basis set to the volume, we perform consecutive calculations (i.e., stop and restart) to fully relax the structure. Reported energies are obtained from a final static calculation.

We test the dependence of energy *differences* among the α- and β-rhombohedral and optimized symmetry-broken β structures on computational parameters. The results are summarized in Table I. To maintain consistent cell sizes we use a $2\times2\times2$ supercell of the α phase, whose lattice parameters become similar to those of the β form. The plane-wave energy cutoff E_{cut} is 319 eV by default, and we also test 415 eV. Precision settings of "medium" and "accurate" set the density of fast Fourier transform grids which control wraparound errors. We systematically increase the Monkhorst-Pack k-point mesh starting from $1\times1\times1$ (i.e., the Γ point) until sufficient convergence is achieved. Based on the data presented, we claim energy differences are converged to within 6% (roughly two significant figures) provided we use a k-point mesh of $3\times3\times3$ and accurate precision. The default plane-wave energy cutoff of 319 eV suffices.

In Table II we test the dependence on choice of potential and exchange-correlation functional. The local density approximation[27] is expected to be the least accurate method. The ultrasoft pseudopotential (USPP) method[28] treats only the valence electrons explicitly. The HARD potential has a very small core radius and correspondingly high E_{cut} =700 eV. Results with this potential are expected to be comparable in accuracy to all-electron full-potential augmented plane-wave calculations (FLAPW) and to Gaussian with large basis sets, according to VASP documentation.[29]

Because our final energy difference $E_{\mathrm{opt}}-E_{\alpha}$ is not much larger than the variation among the GGA calculations, it would be desirable to repeat this calculation using more refined quantum-chemical methods. However, all methods agree that our optimized structure achieves a lower energy than α form, with the exception of the LDA, which is expected to be the least accurate. Even if a more accurate calculation were to find that *all* variants of the β structure were higher in energy than the α, that would not alter our central conclusion that the fully symmetric β-rhombohedral structure is a high-temperature phase stabilized by occupancy fluctuations.

TABLE I. Structural data including atoms per primitive cell, volume (Å^3/atom), and energy relative to α-R (meV/atom). ΔR (Å) measures the deviation of the symmetry-averaged relaxed positions from the crystallographically reported positions, averaged over the fully occupied Wyckoff positions. Comments list occupied sites using notation in . 3. From top to bottom: tetragonal, fully occupied rhombohedral, rhombohedral symmetry-broken structures, and our optimized supercell structure.

Name	Pearson	Atoms	V	$E-E_{\alpha}$	ΔR	Comments
α-T	$tP50$	50	7.67	91.91	0.057	Full occupation
β-T	$tP196$	192	7.53	15.13	0.056	Optimized occupation
β-R	$hR105$	105	7.72	25.87	0.023	Full occupation
α-R	$hR12$	12	7.18	0.00	0.002	Full occupation
β-R	$hR111$	105	7.69	13.02	0.013	B13*bcdef*B16*a*
β-R	$hR111$	106	7.64	0.15	0.012	B13*bcdef*B16*bd*
β-R	$hR141$	107	7.57	−0.86	0.005	B13*bcef*B16*bd*B17*a*B18*a*
β-R	$hR141$	108	7.56	1.43	0.015	B13*bcef*B16*acd*B17*a*B18*a*
$2\times1\times1$	$aP282$	214	7.57	−1.75		Optimized supercell

TABLE II. Test of convergence as function of energy cutoff, VASP precision setting, and k-point mesh. Energies of $hR105$ (E_β) and our optimal B13$bcef$B17aB18a structure (E_{opt}) are compared with that of $hR12$ (E_α).

	$\Delta E=E_\beta-E_\alpha$				$\Delta E=E_{\text{opt}}-E_\alpha$			
	$E_{\text{cut}}=319$ eV		$E_{\text{cut}}=415$ eV		$E_{\text{cut}}=319$ eV		$E_{\text{cut}}=415$ eV	
	Precision							
	Med	Acc	Med	Acc	Med	Acc	Med	Acc
$k=1\times1\times1$	−7.76	−7.54	−7.98	−7.97	−17.27	−17.08	−17.04	−17.15
$k=2\times2\times2$	23.58	23.78	23.85	23.77	−1.71	−1.47	−1.47	−1.68
$k=3\times3\times3$	25.71	25.88	26.09	25.99	−1.05	−0.86	−0.65	−0.85
$k=4\times4\times4$	25.29	25.39	25.65	25.49	−1.04	−0.88	−0.64	−0.87

II. RESULTS

Total energy calculations depend on precise knowledge of atomic positions, with partially occupied sites resolved into a specific pattern of occupied or vacant positions. Likewise, partial site occupancy is thermodynamically forbidden in the $T=0$ K limit. Hence we explore the ensemble of likely instantaneous configurations, seeking both the unique optimal arrangement of atoms among partially occupied sites as well as an estimate of the entropy associated with nearly optimal configurations. We carry out the study initially within a single rhombohedral primitive cell, repeated infinitely owing to the periodic boundary conditions. Later we study superlattice ordering within supercells.

Table III lists our main results.[30] Energies are given relative to the α-rhombohedral form, which we take as a reference because it contains no partial occupancy and was previously the lowest-energy structure that was known. As expected, the tetragonal structures, known to be metastable, exhibit relatively high energies. The fully occupied $hR105$ β-rhombohedral structure is higher in energy than the α-rhombohedral $hR12$ structure, as previously noted.[7–10] If the β form is to be stable at low temperatures it must involve the placement of atoms among the partially occupied sites of $hR111$ or $hR141$. Some particular pattern of occupied and vacant sites must minimize the total energy while breaking the rhombohedral symmetry.

Tables IV and V present energy data supporting specific conclusions on the optimization of $hR111$ and $hR141$. Figures and atomic coordinates for each named structure, and many other structures not listed here, can be viewed at our web site[30] (see the special "published" area). Data are shown for symmetry-inequivalent structures. All energies are given for a $3\times3\times3$ Monkhorst-Pack k-point mesh, for accurate precision and the standard PAW potential with default plane-wave energy cutoff of 319 eV as discussed in Sec. I B.

The notation lists only those sites among the partially occupied Wyckoff positions that are actually occupied. Positions B1–B12, B14, and B15 are always fully occupied and thus are not listed in our notation. The $hR111$ structure introduces partial occupancy at B13 and the new B16 position. The $hR141$ structure introduces additional positions B17–B20. The notation $abcdef$ refers to specific sites within each Wyckoff position, as labeled in Fig. 3.

A. Pearson $hR111$ model

We first explore the $hR111$ model.[18] The two partially occupied sites B13 and B16 are both of Wyckoff type 18h, meaning that $18/3=6$ of these sites occur per rhombohedral primitive cell. The B13 sites form a pair of equilateral triangles surrounding the B15 site at the primitive cell body center (see light blue atoms in Fig. 3). The B16 sites form a pair of equilateral triangles that lie immediately above faces of the icosahedra at primitive cell vertices (see pink atoms in Fig. 2).

A B13 atom can be swapped for a B16 atom in four symmetry-inequivalent ways, each of which lowers the energy by 12–13 meV/atom. This substitution is thus strongly preferred energetically, but the spatial correlation between occupied and vacated site is relatively weak, as suggested by Slack *et al.*[19]

Since the number of atoms per cell is believed to be greater than 105, we also considered a single B13 vacancy and a pair of B16 atoms, again exhaustively testing all combinations. Low energy requires that one atom reside on each equilateral triangle of B16. Our optimal structure within the confines of $hR111$ is $B13bcdefB16bd$, at an energy of 0.15 meV/atom above $hR12$. The $B13bcdefB16bf$ structure was the best found in a previous study by van Setten *et al.*[10]

B. Pearson $hR141$ model

So far the occupancy of B13 is larger than reported experimentally, the energy remains above the energy of the α

TABLE III. Test of alternate potentials. All calculations are done with a $3\times3\times3$ mesh at the default energy cutoff. USPP and HARD use the PW91 GGA. LDA and HARD use PAW potentials.

	$\Delta E=E_\beta-E_\alpha$		$\Delta E=E_{\text{opt}}-E_\alpha$	
	Precision			
	Medium	Accurate	Medium	Accurate
LDA	47.83	47.86	15.48	15.46
USPP	27.82	27.56	−0.25	−0.45
HARD	36.06	25.94	−0.59	−0.75

TABLE IV. Selected data for *hR*111. (Top) Full B13 occupation; (middle) single B13 vacancy with single or double occupation of one B16 triangle; (bottom) single occupancy of both B16 triangles. Energy units are meV/atom.

B13 sites	B16 sites	Atoms	$E-E_\alpha$
a b c d e f		105	25.84
a b c d e f	*a*	106	12.25
a b c d e f	*bd*	107	12.50
b c d e f		104	27.38
b c d e f	*a*	105	13.02
b c d e f	*ab*	106	13.81
b c d e f	*b*	106	13.10
b c d e f	*bd*	106	0.15
b c d e f	*be*	106	5.21
b c d e f	*bf*	106	0.87

form, and the total number of atoms per primitive cell remains below the experimentally reported value of 106.7. Evidently we should try removing another atom from B13 and placing that atom (and more) at other locations. To place these atoms we utilize the additional partially occupied positions of *hR*141, namely, B17–B20. There are of order 10^6 distinct arrangements of atoms within a single primitive cell that are consistent with experimentally observed occupancies. Since this is far too many structures to explore exhaustively, we build upon our prior results and consider other likely correlations in order to focus our search.

Following Slack *et al.*[19] we note that the 1.57 Å bond between B13 and B17 sites is slightly too short for simultaneous occupancy. If we choose to occupy B17*a*, this model suggests that B13*d* and B13*e* should be vacant. However, our calculations show that this arrangement is not stable. One of the vacancies moves to the B13*a* site leaving just a single vacancy on either B13*d* or B13*e* but not both. Then the B17*a* atom relaxes to accommodate the bond to the remaining nearby B13 atom, which ends up at length 1.86 Å. It

TABLE V. Selected data for *hR*141. (Top) B13 vacancies; (middle) B16 occupation; (bottom) structures occupying B19 and B20 sites. Energy units are meV/atom.

B13 sites	B16 sites	B17	B18	B19	B20	Atoms	$E-E_\alpha$
a b c d e f	*bd*	*a*				108	6.62
b c d e f	*bd*	*a*				107	20.29
b c ef	*bd*	*a*				106	0.15
b c ef	*ad*	*a*	*a*			107	−0.07
b c ef	*bd*	*a*	*a*			107	−0.86
b c ef	*cd*	*a*	*a*			107	3.48
b c ef	*bd*			*a*		106	12.96
b c ef	*bd*	*a*	*a*		*h*	108	0.844

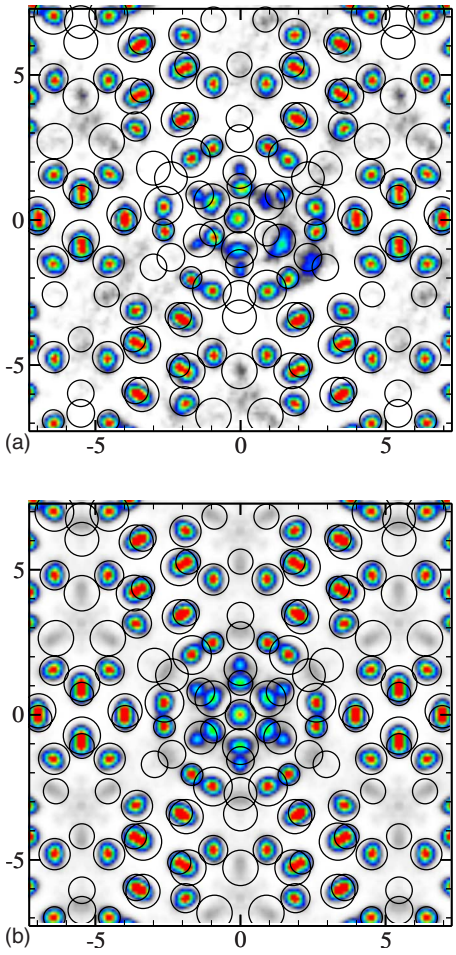

FIG. 4. (Color online) Density plot of simulated atomic positions. Gray scale indicates low-frequency positions, colors indicate medium (blue)–high (red) frequency positions. Crystallographically determined atomic positions are superimposed (and suitably scaled) for comparison with Fig. 3. (a) Run started in optimal configuration. (b) Same data with rhombohedral symmetry imposed by averaging.

is noteworthy that the B17 site reports an anomalously large thermal Debye-Waller factor, indicating large displacements from the refined position. We suggest that this position should be split into distinct sites whose occupancy is correlated with the nearby B13 site. In fact, Slack *et al.* utilized an alternative split site "B17*d*" to refine one of their samples, and one of these "B17*d*" sites lies within 0.1 Å of our relaxed B17 position.

The 1.62 Å bond length between sites B17 and B18 is within the favorable range, and their reported occupancies are similar, so we presume their occupation is correlated. Our calculated energies confirm this, with a reduction in energy of 1.1 meV/atom upon introduction of an atom at the B18 site adjacent to an occupied B17 site. After optimizing the placement of B16 atoms this leads to our optimal primitive cell structure B13*bcef*B16*bd*B17*a*B18*a*, which contains 107 atoms and achieves an energy 0.86 meV/atom below the energy of the α form. This model also achieves a close match of relaxed positions to experimentally observed positions, as is evident from the ΔR values in Table III.

TABLE VI. Hexagonal unit cell energies. Site occupancy is given for each primitive cell (1), (2), and (3). ΔE is relative to a supercell of the optimal 107-atom $hR141$ structure, in units of meV/atom.

B13(1)(2)(3)	B16(1)(2)(3)	B17B18(1)(2)(3)	Atoms	ΔE
(*bcef*) (*bcef*) (*bcef*)	(*bd*) (*bd*) (*bd*)	(*aa*) (*aa*) (*aa*)	321	0
(*bcef*) (*acde*) (*bcef*)	(*bd*) (*cf*) (*bd*)	(*aa*) (*bb*) (*aa*)	321	0.09
(*bcef*) (*acde*) (*abdf*)	(*bd*) (*cf*) (*ae*)	(*aa*) (*bb*) (*cc*)	321	0.31

The B19 and B20 sites so far remain unused in our study. B19 sites are only 0.74 Å away from B18 sites, so these may never be simultaneously occupied. Both B19 and B20 sites lie close to the centers of fully occupied hexagonal rings, resulting in small patches of triangular lattice that are atypical of crystalline boron structures (although they may be stable in small boron clusters and nanotubes[31]). We found no significantly low-energy structures utilizing B19 or B20 sites. Van Setten *et al.*[10] report a low energy for B19*bcdef*B16*e*B19*a*, but we find this is not favorable. Rather the B19*a* atom relaxes to the nearby B17*a* position.

C. Molecular dynamics

Because we cannot systematically evaluate all configurations within the $hR141$ primitive cell, we checked our result using molecular dynamics. We used the VASP-calculated forces to perform molecular dynamics simulations of a single primitive cell of the β form. To achieve atomic diffusion we employed a high temperature $T=2000$ K (melting is around $T=2365$ K). We estimated the lattice parameters as $a=11.047$ Å and $c=24.155$ Å based on an experimental report of thermal expansion.[32]

We ran samples of 106, 107, and 108 atoms for a duration of 16 ps each, using 1 fs time steps. To search for optimal configurations we drew instantaneous configurations from the molecular dynamics run every 2 ps and quenched them. To carry out the quench we rescaled the lattice parameters to their crystallographic values and performed molecular dynamics simulations with a linearly decreasing temperature ramp that reached $T=300$ K after 3 ps. We then performed conjugate gradient relaxation to reach 0 K. This procedure was able, on occasion, to achieve the optimal structures we reported, but usually resulted in higher energies.

Figure 4 shows a density plot of atomic positions for the 107-atom run that started with our optimal structure as an initial condition. Densities have been averaged to impose rhombohedral symmetry. Sharing of atoms between B13 and B17 positions is clearly visible, as is partial occupation of B18 and B16 positions.

D. Supercell studies

Although we optimized the assignment of partial occupancy within a single $hR141$ primitive cell, there is a possibility of a lower-energy structure within either the hexagonal unit cell (Pearson type $hP423$) or some other supercell of the primitive cell.

The hexagonal unit cell (Pearson type $hP423$, dimensions $a=10.9$ Å, $c=23.8$ Å) contains three copies of the rhombohedral primitive cell stacked in the direction parallel to the rhombohedral (111) axis. We consider the case where each primitive cell is identically decorated, where one is rotated by 120° relative to the other two, and where each is rotated by 120° relative to its neighbors. In this last case a 3_1 screw axis is introduced. In Table VI energies are given for a $3\times3\times1$ k-point mesh with medium precision, maintaining a uniform reciprocal space density comparable to a $3\times3\times3$ mesh for a single primitive cell. It appears energetically preferable to maintain identical orientations of all vertically stacked cells.

However, within a $2\times1\times1$ supercell of the 107-atom primitive cell, which places independent primitive cells adjacent to each other (see Fig. 5), we did find superstructures that lowered the energy significantly. To describe these we focus on a motif near the center of our optimal primitive cell structure. One of the two B13 vacancies is collinear with the occupied B17 and B18 sites (e.g., B13*a*B17*a*B18*a*). The second B13 vacancy is adjacent to the first (e.g., B13*d*). This motif of collinear and adjacent sites can occur in six rotated variants and six more that are reflected versions.

We examined all 22 symmetry-inequivalent arrangements of this motif within the 214-atom supercell. For each arrangement we optimized the placement of the B16 atoms. The relative arrangements are coupled mainly by the placement of B16 atoms, and all energies lie within 2 meV/atom of each other. Energies are given in Table VII for a $1\times3\times3$ k-point mesh and precision set to accurate. Several supercell structures yielded energies lower than that of the op-

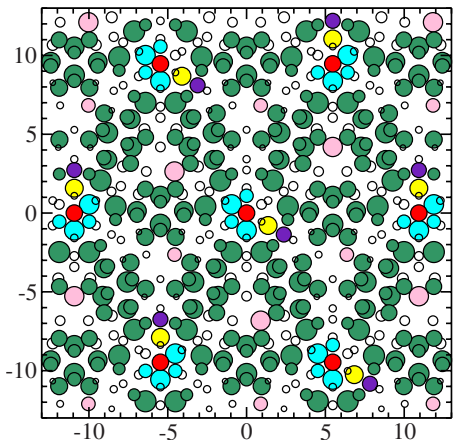

FIG. 5. (Color online) Optimal site occupation of a β-rhombohedral $2\times1\times1$ supercell viewed along the rhombohedral (111) axis. Color coding as in Figs. 2 and 3. Small empty circles locate vacant sites.

timal 107-atom structure, indicating a preference for superlattice ordering at low temperatures, with adjacent cells of the β structure resolving their partial occupancy with differing orientations of a common motif.

The large number of nearly degenerate configurations suggests the possibility of a phase transition from the symmetry-broken low-energy structure to a state that restores the β-rhombohedral symmetry by sampling the full ensemble of motif orientations. To judge the chance of such a phase transition, we evaluate the partition function of our $2\times1\times1$ supercell

$$Z=\sum_{\alpha}\Omega_{\alpha}e^{-E_{\alpha}/k_BT}, \tag{1}$$

where α runs over all 22 symmetry-independent configurations, Ω_{α} is the multiplicity of the configuration, and E_{α} is the relaxed energy, optimized over placements of B16 atoms (as in Table VII but multiplied by 214 for the number of atoms per supercell).

Thermodynamic derivatives of Z yield the internal energy U, the entropy S, and the heat capacity C. The heat capacity exhibits a strong peak around $T=300$ K. Figure 6 plots thermodynamic data resulting from this model. The strong peak around $T=300$ K represents the unlocking of the relative orientations of our collinear motif (see above). The small heat capacity peak around $T=50$ K represents the unlocking of the second B13 vacancies (see above) while the collinear motif is held fixed. The entropy available from unlocking dominates the energy cost, substantially lowering the free energy. Based on this, it seems likely that in an infinite system there should be a symmetry-restoring phase transition at a moderate temperature, driven by the entropy of suboptimal occupation patterns of the partially occupied sites. This transition may be difficult to observe experimentally because atomic diffusion is slow at this temperature.

III. DISCUSSION

The symmetry space group of β-rhombohedral boron is $R\bar{3}m$ (group no. 166). To preserve rhombohedral symmetry in the primitive cell, every Wyckoff position must be fully occupied or fully vacant. If the favored structure occupies only a subset of the sites in one or more Wyckoff position, the symmetry is necessarily lower. Our optimal vacancy-ordered structure within the primitive cell yields space group $P1$ (group no. 1) corresponding to no point symmetry whatsoever.

According to Landau theory[33] changes of symmetry occur through thermodynamic phase transitions, implying that the β-rhombohedral structure is not the low-temperature stable phase. Experimental observation of β as stable indicates either that vacancies are frozen in a disordered arrangement or that β is stabilized by a symmetry-restoring phase transition at some low temperature. This conclusion holds regardless of whether we have found the true optimal structure, since all energetically plausible variants of β lack full symmetry.

The transition temperature is only a crude estimate because of several approximations. We consider only the coupling of two primitive cells. We consider only a small fraction of all configurations within these two cells. We neglect atomic vibrations, which contribute strongly to the free energy,[7,10] and must be included in any attempt to estimate an accurate transition temperature. However, while the α and β phases differ strongly in vibrational free energy, the ensemble of nearly optimal symmetry-broken β variants most likely remains nearly degenerate in vibrational free energy because their local environments are so similar.

Because our calculated energy differences are at the borderline of reliability of density functional methods, it would be desirable to study these energies using more sophisticated quantum-chemical methods. Unfortunately, at present these methods cannot be reliably applied to periodically repeated crystal structures of the necessary complexity. Although details of the optimal structures may change, our primary conclusions are unlikely to be altered by higher accuracy. The true ground state will be either the symmetry-broken β or perhaps the α state. In either case a phase transition is necessary to recover the experimentally observed equilibrium state above some moderate temperature.

Even within the density functional theory limitations, there remains some uncertainty concerning the optimal structure. Within a single primitive cell we have explored only a fraction of all configurations, and some other unexamined structure might turn out to be preferred. Among supercells we have addressed only the hexagonal unit cell and the $2\times1\times1$ supercell. It is quite possible that a larger supercell

TABLE VII. Selected $2\times1\times1$ supercell energies, including multiplicities Ω. ΔE is relative to a doubling of the optimal 107-atom $hR141$ structure, in units of meV/atom.

B13(1)(2)	B16(1)(2)	B17B18(1)(2)	Ω	ΔE
(*bcef*) (*acde*)	(*ad*) (*bd*)	(*aa*) (*bb*)	8	−0.89
(*bcef*) (*acef*)	(*ad*) (*bd*)	(*aa*) (*bb*)	4	−0.75
(*bcef*) (*bcdf*)	(*ce*) (*ad*)	(*aa*) (*ee*)	8	−0.24
(*acde*) (*bcdf*)	(*bd*) (*ad*)	(*bb*) (*ee*)	8	−0.11
(*bcef*) (*bcef*)	(*bd*) (*bd*)	(*aa*) (*aa*)	12	0.00

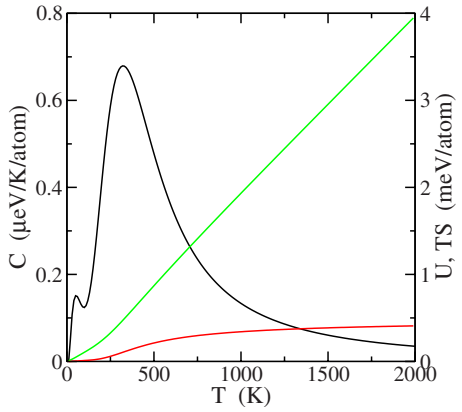

FIG. 6. (Color online) Heat capacity (black), energy (red), and entropy (green) of supercell model. Energy is relative to the optimal supercell structure.

will be even more favorable. In fact, it could be that the true ground state even restores rhombohedral symmetry, though in a supercell so that it is no longer the β structure.

Other studies[7,10] have addressed the paradox that the calculated energy of the β structure exceeds the energy of the α,[8] seemingly in conflict with experimental observation of β as the stable form. Both proposed explanations rely on the differing vibrational properties of the two structures, with the β form exhibiting a higher density of low-frequency modes than the α. The first suggestion[7] noted that the β structure has higher vibrational entropy than the α and suggested that vibrational entropy could stabilize the β form above a high temperature, estimated as $T=970$ K. The second suggestion[10] utilized some of the partially occupied sites to bring the energy of the β phase nearly down to the level of the α form. The remaining energy difference could be compensated by quantum zero-point vibrational energy, potentially explaining the stability of the β form at temperature $T=0$ K. In contrast, our results optimize the assignment of partially occupied sites in the β form, bringing the energy below α. While we concur that vibrational effects further stabilize the β phase, they are not needed to explain the stability relative to α.

In conclusion, we show that suitably resolving correlations among partially occupied sites of the β form yields an optimal structure whose energy is lower than α. This structure breaks the symmetry of the β structure because it uses only subsets of the fully symmetric Wyckoff positions. Further, we demonstrate the likelihood of superlattice ordering. We propose that the full symmetry of the β form is restored at moderate temperatures through a phase transition driven by the entropy of partial site occupation.

ACKNOWLEDGMENTS

This research was supported in part by the NSF under Grant No. DMR-0111198. We acknowledge useful discussions with B. Widom.

[1] J. L. Hoard, S. Geller, and R. E. Hughes, J. Am. Chem. Soc. **73**, 1892 (1951).
[2] J. L. Hoard, R. E. Hughes, and D. E. Sands, J. Am. Chem. Soc. **80**, 4507 (1958).
[3] L. V. McCarty, J. S. Kasper, F. H. Horn, B. F. Decker, and A. E. Newkirk, J. Am. Chem. Soc. **80**, 2592 (1958).
[4] B. F. Decker and J. S. Kasper, Acta Crystallogr. **12**, 503 (1959).
[5] R. E. Hughes, C. H. L. Kennard, D. B. Sullenger, H. A. Weakliem, D. E. Sands, and J. L. Hoard, J. Am. Chem. Soc. **85**, 361 (1963).
[6] M. Vlasse, R. Naslain, J. S. Kasper, and K. Ploog, J. Solid State Chem. **28**, 289 (1979).
[7] A. Masago, K. Shirai, and H. Katayama-Yoshida, Phys. Rev. B **73**, 104102 (2006).
[8] M. Mihalkovic and M. Widom, Phys. Rev. B **70**, 144107 (2004).
[9] D. L. V. K. Prasad, M. M. Balakrishnarajan, and E. D. Jemmis, Phys. Rev. B **72**, 195102 (2005).
[10] M. J. van Setten, M. A. Uijttewaal, G. A. de Wijs, and R. A. de Groot, J. Am. Chem. Soc. **129**, 2458 (2007).
[11] H. Werheit and R. Franz, J. Less-Common Met. **117**, 163 (1986).
[12] H. C. Longuet-Higgins and M. de V. Roberts, Proc. R. Soc. London, Ser. A **230**, 110 (1955).
[13] W. N. Lipscomb, J. Less-Common Met. **82**, 1 (1981).
[14] E. D. Jemmis and M. M. Balakrishnarajan, J. Am. Chem. Soc. **123**, 4324 (2001).
[15] A "Wyckoff position" is a group of symmetry-equivalent atomic sites.
[16] D. Geist, R. Kloss, and H. Follner, Acta Crystallogr., Sect. B: Struct. Crystallogr. Cryst. Chem. **26**, 1800 (1970).
[17] J. L. Hoard, D. B. Sullenger, C. H. L. Kennard, and R. E. Hughes, J. Solid State Chem. **1**, 268 (1970).
[18] B. Callmer, Acta Crystallogr., Sect. B: Struct. Crystallogr. Cryst. Chem. **33**, 1951 (1977).
[19] G. A. Slack, C. I. Hejna, and J. S. Kasper, J. Solid State Chem. **76**, 52 (1988).
[20] G. Kresse and J. Furthmuller, Phys. Rev. B **54**, 11169 (1996).
[21] P. E. Blochl, Phys. Rev. B **50**, 17953 (1994).
[22] G. Kresse and D. Joubert, Phys. Rev. B **59**, 1758 (1999).
[23] J. P. Perdew and Y. Wang, Phys. Rev. B **45**, 13244 (1992).
[24] I. Boustani, Chem. Phys. Lett. **233**, 273 (1995).
[25] B. Marlid, K. Larsson, and J.-O. Carlsson, Phys. Rev. B **64**, 184107 (2001).
[26] I. Boustani, Phys. Rev. B **55**, 16426 (1997).
[27] D. M. Ceperley and B. J. Alder, Phys. Rev. Lett. **45**, 566 (1980).
[28] D. Vanderbilt, Phys. Rev. B **41**, 7892 (1990).
[29] http://cms.mpi.univie.ac.at/vasp/vasp/node239.html
[30] See http://alloy.phys.cmu.edu/published for energetic and structural details.
[31] S. Chacko, D. G. Kanhere, and I. Boustani, Phys. Rev. B **68**, 035414 (2003).
[32] T. Lundstrom, B. Lonnberg, and J. Bauer, J. Alloys Compd. **267**, 54 (1998).
[33] L. D. Landau and E. M. Lifshitz, *Statistical Physics* (Pergamon, Oxford, 1969).